

On semi-empirical decomposition of multidecadal climate variability into

forced and internally generated components

Sergey Kravtsov and David Callicutt

Department of Mathematical Sciences, Atmospheric Science Group, University of Wisconsin-Milwaukee, P.O. Box 413, Milwaukee, WI 53201

Session: A23G: Grand Challenges in Earth System Modeling: Decadal Climate Variability and Change, Prediction, and Its Applications

Presentation number: A23G-0300 ; Display time: Tuesday, December 13th; 1:40 PM - 6:00 PM

Introduction

State-of-the-art global coupled climate models used to simulate 20th century climate use similar dynamical cores, but differ in details of the forcing and in the parameterizations of unresolved subgrid-scale physical processes (Taylor et al. 2012). We considered 18 independent ensembles of the CMIP5 model simulations (with the total of 116 simulations) for attribution of the 20th century climate change.

Data sets and methodology

We extracted, from CMIP5 model simulations and observations, a set of sea-surface temperature (SST) and sea-level pressure (SLP) based climate indices representing regional and hemispheric climate variability over the course of the 20th century. These indices included the well-known AMO and NAO indices, as well as the PMO index defined by Steinman et al. 2015 (an analogue of the AMO index for the Pacific). We also considered the NMO index (the Northern Hemisphere mean surface air temperature).

Climate model simulations match the non-uniform warming of NMO very well, but are overly sensitive to forcing in the North Atlantic and North Pacific regions, where the models' historical simulations have to be scaled back to match the observed trends (Fig. 1). We estimated the forced signals in the individual models via the 5-yr low-pass filtered ensemble mean (SMEM) and computed the residual time series of internal variability in each simulation. We further used a linear stochastic model to produce synthetic Monte Carlo 'CMIP5' ensembles and to compute the time-scale-dependent biases and uncertainties of our forced and internal variability estimates.

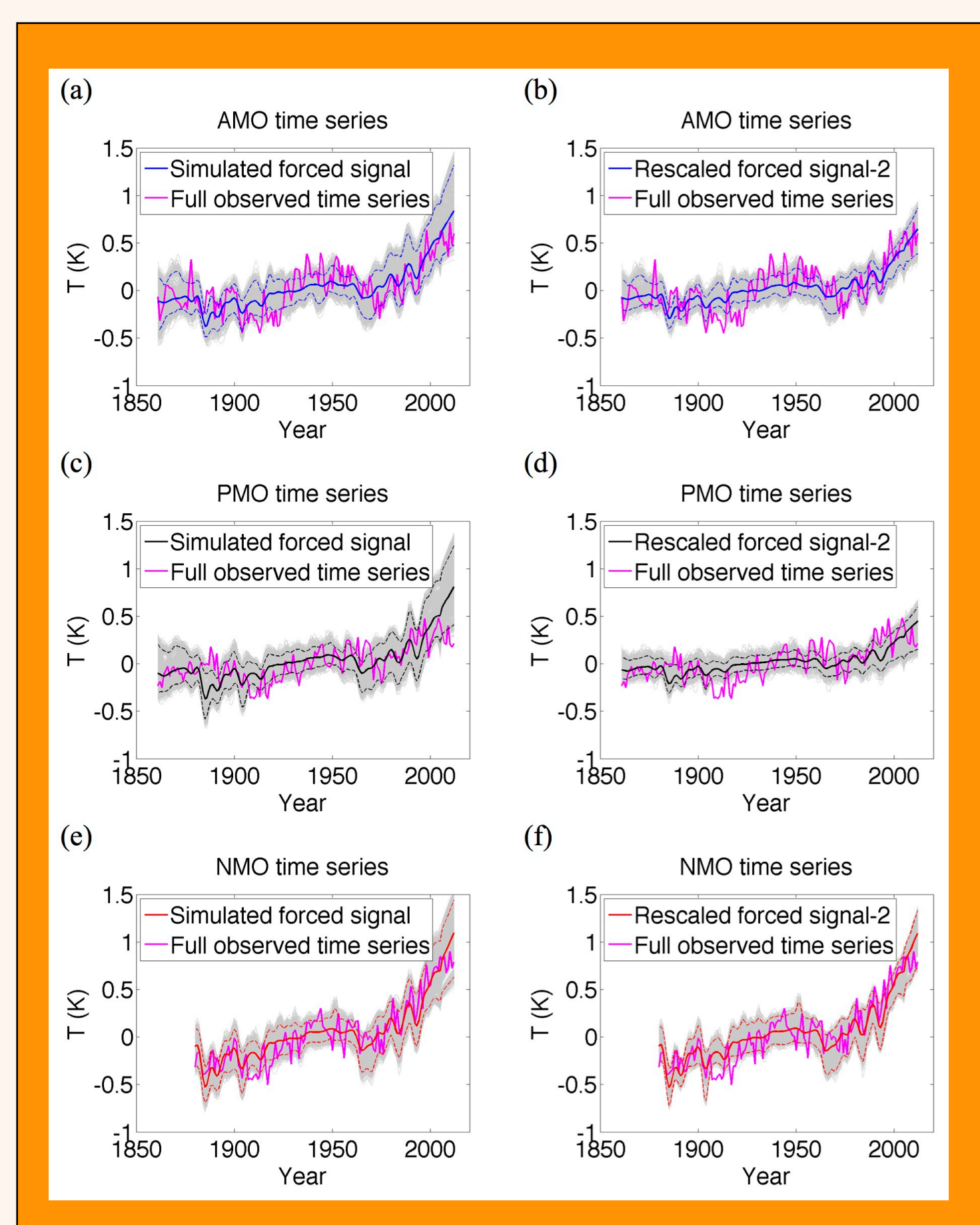


Fig. 1: Estimated forced signals and their uncertainties for the AMO (a, b), PMO (d, e) and NMO (g, h) time series obtained via SMEM-based Monte Carlo method applied to the multi-model ensemble of twentieth-century simulations. Magenta lines show the observed time series. The solid and dashed colored lines show the ensemble-mean and the 95% spread of the individual forced-signal estimates. Left: non-scaled forced signals. Right: signals rescaled to match observations.

Multidecadal climate variability

Differencing the observed time series (purple lines in Fig. 1) and our surrogate forced-signal estimates (gray lines in Fig. 1) produces the corresponding surrogate estimates of the observed internal variability. The ensemble-mean estimates of the multidecadal (40-yr low-pass filtered) internal variability in AMO, PMO and NMO in Fig. 2 are broadly similar to those in Steinman et al. (2015), but their uncertainty is much larger than these authors have implied. In particular, this uncertainty is sufficiently large to render the attribution of the recent cool down of the PMO (Fig. 2c) and NMO (Fig. 2e) to the internal variability barely statistically significant if at all.

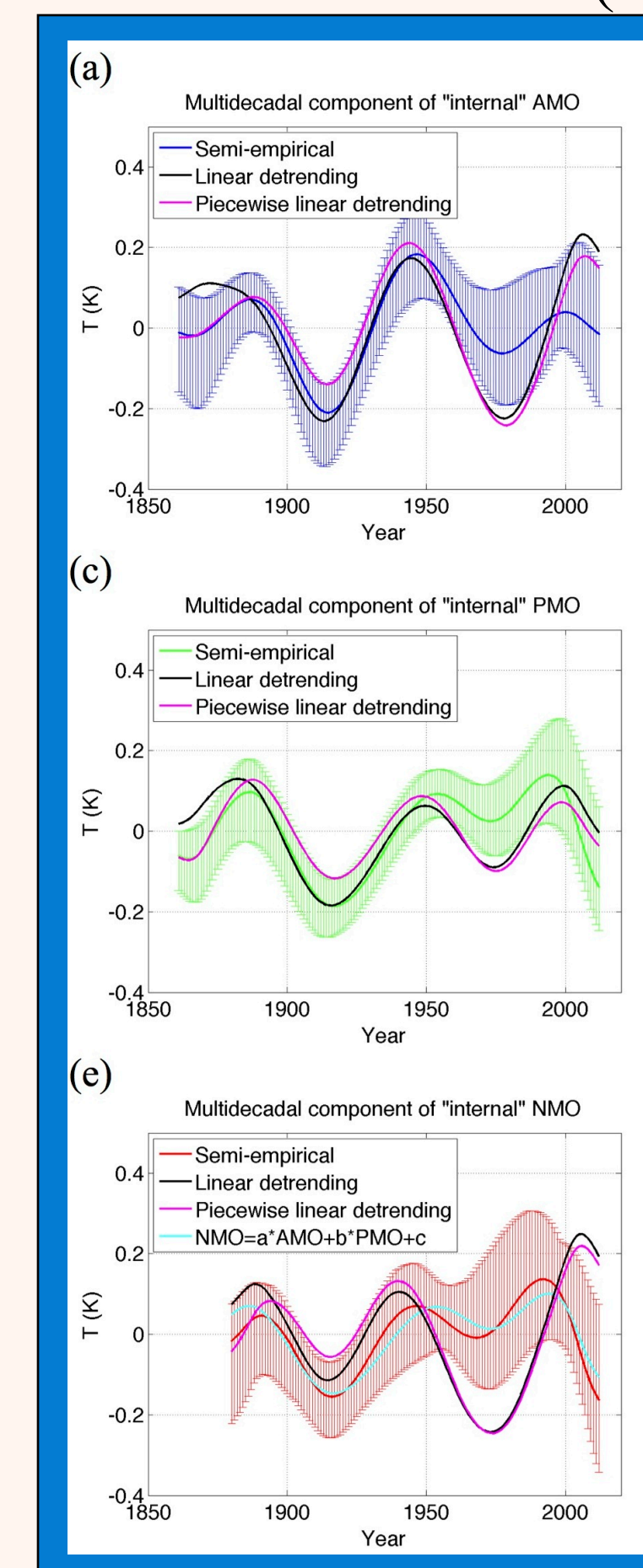


Fig. 2: Estimates of observed multidecadal intrinsic variability for AMO (a), PMO (c) and NMO (e). These estimates were obtained using the rescaled forced signals in Fig. 1 (right). These rescaled forced signals were subtracted from the corresponding observed time series, 40-yr low-pass filtered and windowed using the appropriate tapers to minimize end effects. Heavy solid colored lines (AMO: blue, PMO: green, and NMO: red) show the ensemble mean of the resulting intrinsic signal estimates, and error bars — their 95% spread. Each panel also contains for reference the "internal" estimates based on subtracting linear trend from the entire observed time series, as well as the one based on the piecewise linear detrending with the break point at 1900.

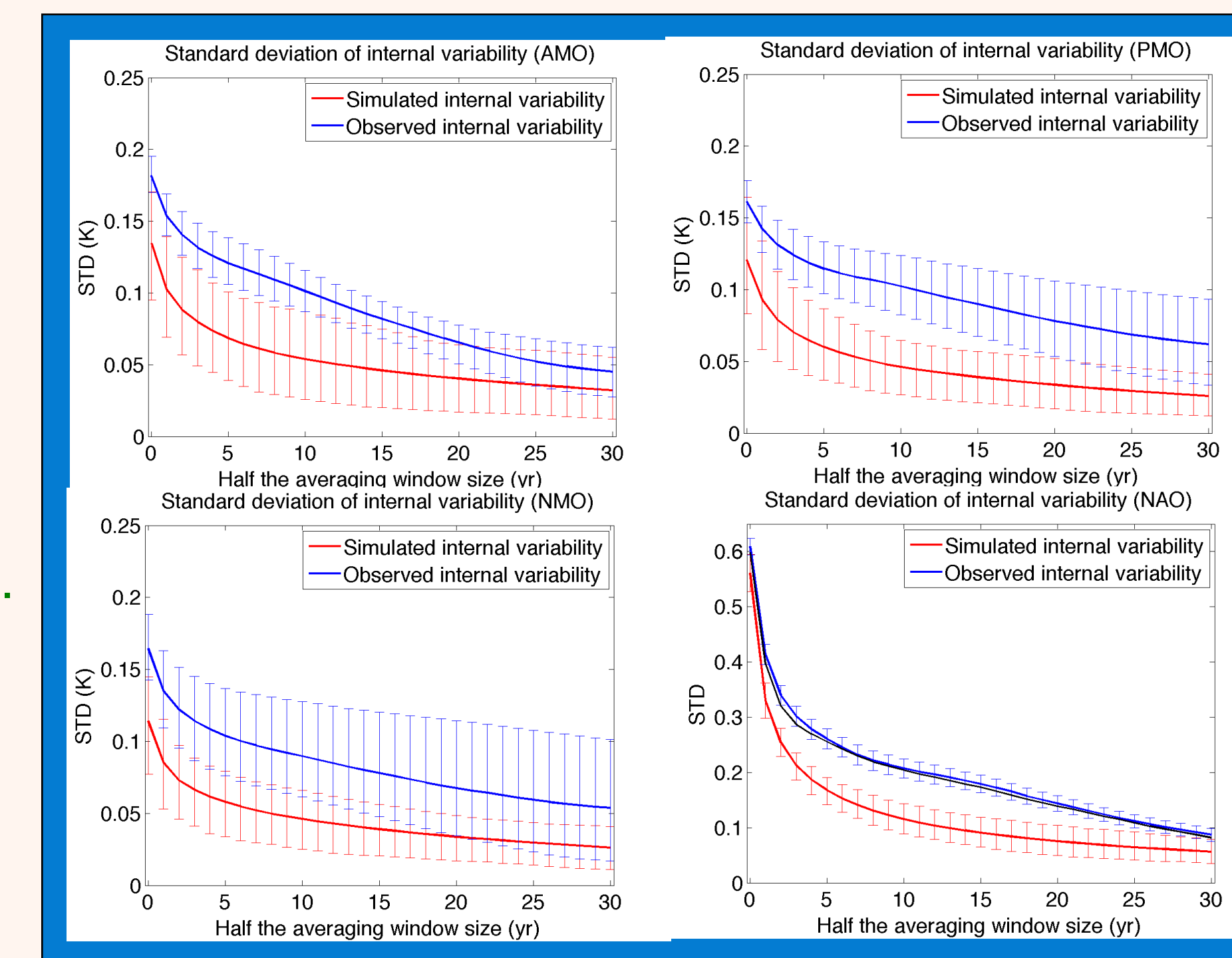


Fig. 3: Standard deviations (STD) of the observed (blue) and CMIP5 simulated (red) internal variability in the AMO, PMO, NMO and NAO indices. STD were computed for raw and low-pass filtered time series (abscissa shows half the averaging window size for the latter). The STDs of model simulated internal

variability were multiplied by inflation factors (not shown) derived from our Monte Carlo simulations. Heavy lines — ensemble-mean STD, error bars — the 67% spread (standard uncertainty) of the STD estimates based on individual model simulations.

Figure 3 demonstrates that internal decadal+ time scale variability simulated by the CMIP5 models is significantly weaker than the observed internal variability inferred by subtracting the rescaled CMIP5 derived forced signals from the full observed climatic time series. This is despite the observed internal variability so defined has minimum possible amplitude (since the model based forced signals are rescaled to minimize the residual variance) and despite that the simulated internal variability was scaled up to correct for aliasing some of the true internal variance into the estimated smoothed SMEM-based forced signal.

This difference in magnitude of the observed vs. simulated internal variability can be attributed to a low-dimensional spatiotemporal mode brought out by the Multi-channel Singular Spectrum Analysis (M-SSA: Ghil et al. 2002) of the (normalized) internal components of the observed and simulated AMO/PMO/NMO/NAO/ALPI multivariate time series (Fig. 4). This mode in observations is associated with the leading M-SSA pair, which stands out prominently above the rest of the M-SSA spectrum. On the other hand, the M-SSA spectra of CMIP5 model simulations are flat, and the leading observed M-SSA pair dominates the differences between the observed and simulated spectra.

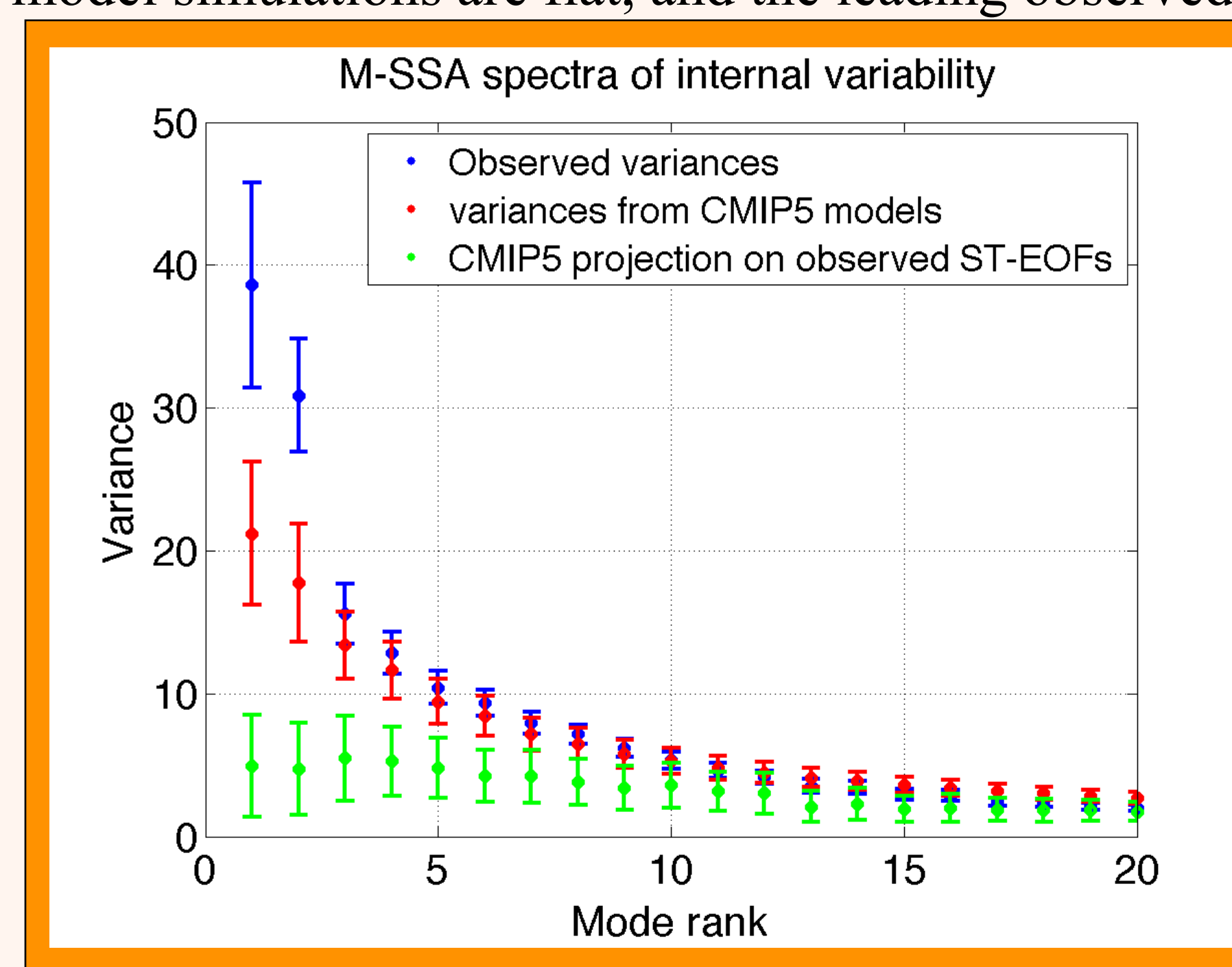


Fig. 4: M-SSA spectrum of the observed (blue) and simulated (red) internal variability. The green error-bar plot shows variances obtained by projecting the simulated internal variability onto the observed ST-EOFs of M-SSA analysis.

Furthermore, projecting the model simulated climate indices onto the space-time patterns of the observed M-SSA modes results in a very small magnitude of the associated variability, especially for the leading M-SSA pair; thus, models lack the spatiotemporal structures which characterize this mode. If we subtract the leading M-SSA pair from the observed and simulated internal variability, the differences in variance between the observed and simulated internal signals (Fig. 3) is greatly reduced (Fig. 5).

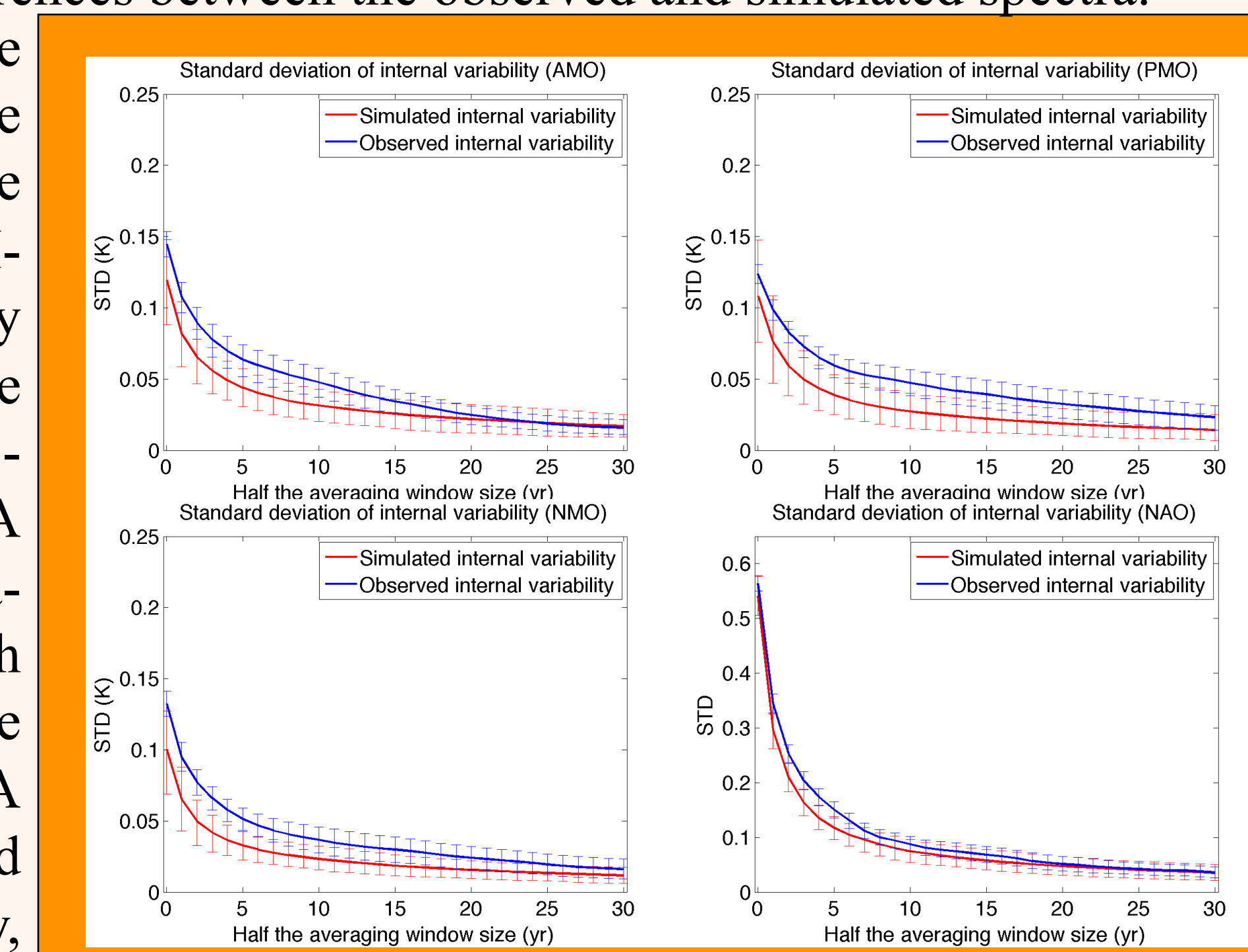


Fig. 5: The same as in Fig. 3, but for the STDs of internal variability from which the component associated with the leading M-SSA pair (Fig. 4) was subtracted.

Discussion

The most striking result of our study is the demonstration that the CMIP5 simulated internal variability in SST and SLP is much weaker than observed. This difference comes from the models' lacking a coherent multidecadal mode which dominates the estimated internal component of the observed internal variability. These discrepancies suggest that a contribution of multi-decadal internal climate variability to the observed climate change is distorted in the CMIP5 simulations; hence, our ability to attribute and predict climate change using the current generation of climate models is limited.

On one hand, the model-data differences may reflect the uncertainty in modeling the indirect aerosol effect on climate (Booth et al. 2012; Golaz et al. 2013), with models possibly underestimating the multidecadal component of the true forced climate response. Alternatively, climate models may misrepresent some of the dynamical feedbacks hypothesized by the authors of this poster to be responsible for the hemispheric propagation of the AMO-type multidecadal signal (Wyatt et al. 2012; Kravtsov et al. 2014), in which case the model-data differences would reflect the lack of multidecadal internal dynamics in climate models.

References

- Booth, B. B. B., et al., 2012. *Nature*, **484**, 228–232.
- Ghil, M., et al., 2002. *Reviews of Geophysics*, **40**, 1003.
- Golaz, J.-C., et al., 2013. *Geophys. Res. Lett.*, **40**, 2246–2251.
- Kravtsov, S., et al., 2014. *Geophys. Res. Lett.*, **41**, 6881–6888.
- Steinman, B. A., et al., 2015. *Science*, **347**, 988–991.
- Taylor, K. E., et al., 2012. *Bull. Am. Meteorol. Soc.*, **93**, 485–498.
- Wyatt, M. G., et al., 2012. *Clim. Dyn.*, **38**, 929–949.

Acknowledgments

We acknowledge the World Climate Research Programme's Working Group on Coupled Modeling, which is responsible for CMIP, and we thank the climate modeling groups for producing and making available their model output. This research was supported by the NSF grants OCE-1243158 and AGS-1408897.

For further information

Please contact kravtsov@uwm.edu. A PDF version of this poster can be found at the Sergey Kravtsov's UWM website — <https://people.uwm.edu/kravtsov/presentations/>